land

Supplemental 1: Methods Supplemental for Knight et. al, 2021

1. Selection, creation, and preparation of the Geographic Base Layers of the Habitat Condition Index

National Land Cover Data (NLCD) for the year 2011 was used as the foundation for this analysis. We first extracted natural lands (those not classified by the NLCD as "Developed" or "Cultivated Crops") from the conterminous United States. Range (excluding hay and pasture) and silvicultural lands were included as natural lands.

Within these lands, multiple anthropogenic stressors, fragmentation, proximity to aquatic habitat, and departure from pre-European conditions were quantified. Each of these categories were then used as inputs to spatially map fragmentation, anthropogenic stressors, proximity to aquatic habitat, and an estimate of the cultivated landscape with structural similarities to paired natural habitats.

1.1 Anthropogenic stressors

Human land uses interact with ecological processes, resulting in habitat degradation [1]. It is generally assumed that ecosystems devoid of human modification of habitat have higher integrity and thus are likely to have higher biodiversity [2,3]. Many published methods for assessing the effects of the relative ecological condition of landscapes within proximity to anthropogenic sources and disturbances have been proposed. The most commonly measured impacts are from roads and utility corridors. Roads cause habitat destruction, land degradation through edge effects, population isolation, and increased mortality [4–9]. Infrastructure creation and use also increases the risk of collisions with various species and stresses breeding due to increased noise and visual stimuli [10–14]. Other types of infrastructure, including railways, power lines, pipelines, hydroelectric projects, oil wells, seismic lines, and wind parks, have been shown to negatively impact biodiversity [15–20].

Building on this multi-decadal foundation of research, this analysis adopts the methods proposed by Hak and Comer [21] to map layers of anthropogenic influence. By combining an impact score with a distance decay, single continuous surfaces are mapped representing the following anthropogenic stressors relating to transportation and urban development listed in Table S1. Hak and Comer [21] provide a repeatable design that is empirically validated from biodiversity data. Transportation input layers will be derived from TIGER roads data (ww.census.gov/geo/maps-data/data/tiger.html) and the urban development layers will use NLCD development classifications. For each input layer where the land use feature occurs, a site impact score is assigned. The Euclidean distance for each input layer is calculated for the model extent with a distance extending away from each feature assigned a site impact score representing the distance decay function. Features assigned a high decay score result in a surface where the impact value decreases within a relative short distance, whereas those locations where a low decay score create surfaces where the per pixel value dissipates much more slowly. The combination of the site impact score and the distance decay value are combined into the formula:

$$f(d) = \prod_{1}^{n} \left(\frac{1}{1 + EXP\left(-2 * \left(d - \frac{(d_s * 0.5)}{d_s * 0.25}\right)\right)} \right)^{(-0.25 * LN(S_i) - 8 * 10 - 16)}$$

where, d is the distance from the feature, d_s is the distance intensity threshold, S_i is the site intensity threshold, and constants as a ration (0.5, 0.25) are added to mark the midpoint and inflection points of the curves at ¼. 1/3, and ¾ points of the curve [21].

Mapped values for each indicator (4 transportation and 3 development) are then summed for each pixel location to provide an estimate anthropogenic influence. While no clear consensus on the distances when anthropogenic sources no longer influence

biodiversity, we chose to adopt the methods developed by Hak and Comer [21] given the rigorous empirical calibration and validation across the conterminous US.

Table S1. Functions and Decay Curves for HCI Components. For the components of the HCI, we determined intensity of impacts and distance decay curves. These parameters, determined through assessing the best available peer-reviewed research on the topic, were then used to create CONUS-wide surfaces depicting each of these components.

		Theme	Intensity Threshold	Decay Score	Impact decays to zero
Natural Lands					
Among	Function	*Transportation*			
		Dirt roads	0.70	0.5	200m
		Local roads	0.50	0.5	200m
		Secondary and connecting roads	0.20	0.2	500m
		Primary Highways	0.05	0.1	1,000m
		Urban and Industrial development			
		Low Density Development	0.60	0.5	200m
		Medium Density Development	0.50	0.5	200m
		High density development	0.50	0.05	2,000m
		Proximity to aquatic resources			
		Distance to water	1.00	0.5	1,000m
	Structure	*Landscape context*			
		Fragmentation	1.00	Figure 4	***
Within	Structure/ Composition	*Departure from historic conditions*			
		Vegetation departure index	1.00	0	***
Cultivated Lands					
Among	Function	*Transportation*			
		Dirt roads	0.70	0.5	200m
		Local roads	0.50	0.5	200m
		Secondary and connecting roads	0.20	0.2	500m
		Primary Highways	0.05	0.1	1,000m
		Urban and Industrial development			
		Low Density Development	0.60	0.5	200m
		Medium Density Development	0.50	0.5	200m
		High density development	0.50	0.05	2,000m
		Proximity to aquatic resources			
		Distance to water	1.00	0.5	1,000m
	Structure	*Landscape context - Fragmentation*			
		1) Tree crop (e.g. orchard) 2) Shrub crop (e.g. huckleberry) 3) Perennial herbaceous crop (e.g. hay) 4) Annual row crop (e.g. corn) 5) Flooded row crop (e.g. rice)	1.00	Figure 5	***
Within	Structure	*Structural similarity*			
		1) Tree crop - NLCD Forest 2) Shrub crop - NLCD Shrub/scrub 3) Perennial herbaceous crop - NLCD Grassland/herbaceous 4) Flooded - NLCD Wetland	1.00	*focal statistic*	1,000m

**** indicates that the indicator provides a value for each cell and does not use a distance decay function.*

1.2. Fragmentation

Landscape modification, primarily from development expanding into natural habitats, has caused increasing fragmentation and been extensively studied [22]. Habitat fragmentation is widely viewed as a negative impact on virtually all taxonomic groups, including birds and mammals [23,24], reptiles and amphibians [25], invertebrates [26] and plants [27]. Focus on quantifying fragmentation has centered largely on forest vegetation and their connectivity. Traditional metrics used as proxies for quantifying fragmentation include forest patch size, percent interior forest, mean forest patch density, number of forest patches, inter-patch distance, forest patchiness, and contiguity [28–33].

We used the Graphical User Interface for the Description of Objects and their Shapes Toolbox (GUIDOS Toolbox), specifically the morphological spatial pattern analysis (MSPA), to segment the natural and cultivated lands for identifying mutually exclusive morphometric feature classes describing the shape, connectivity, and spatial arrangement. The MSPA divided natural and cultivated lands by separating core and non-core areas based on an assumed edge width (90 meters). All of the non-core areas are considered some type of edge, with the MSPA labeling each pixel according to the structural role it

plays with respect to one or more core areas. The results of MSPA allowed for multiple fragmentation categories to be identified, including perforation, bridge, loop, and branch categories (Figure S1). The edge category encompasses a core area (exterior edge) or encompasses a hole in a core area (perforation). A loop is defined as an edge that connects to the same core area twice; a bridge is an edge that connects two or more disjunct core areas; branch is an edge that does not connect to anything.

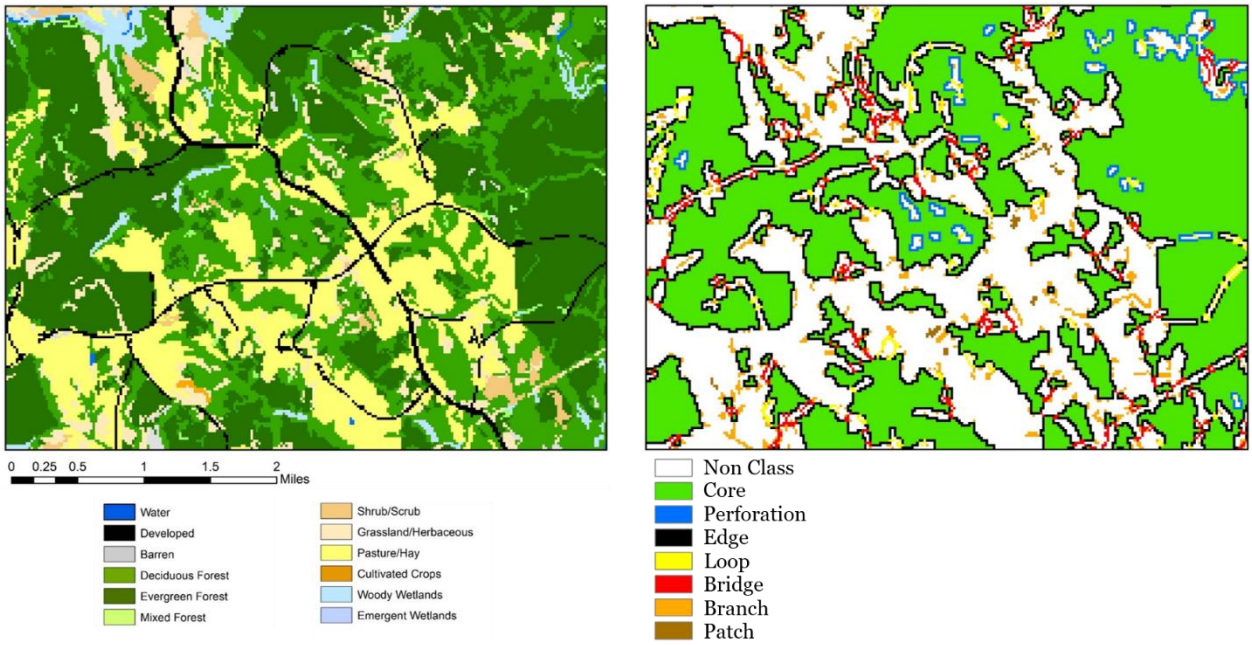

Figure S1. Partitioning by the MSPA for forest classes within a NLCD map (left) into the different fragmentation classes (right).

Following the methods outlined in Hurd et al., [34], we adapt a modified index weighting scheme to incorporate the additional fragmentation categories provided by Guidos Toolbox. Following classification of each pixel into a fragmentation class, the indicator index is assigned to each pixel following the weights in Figure S2. For this work, we used a binary classification of natural and unnatural vegetation. This means that a grassland residing adjacent to a forest pixel were assigned the same binary classification value.

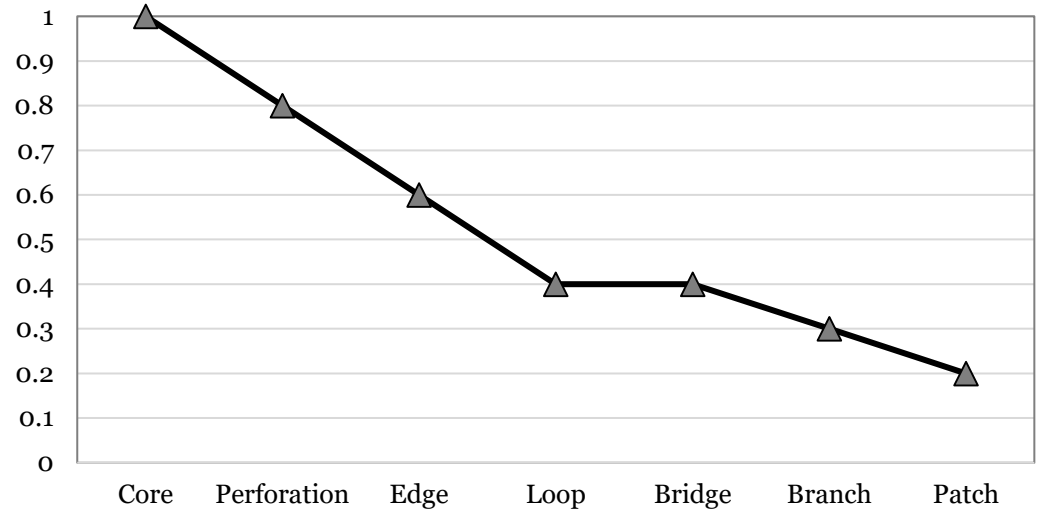

Figure S2. Fragmentation categories and the index weighting values assigned for each category of pixels classified natural vegetation.

1.3. Vegetation departure

To determine vegetation conditions of pre-European settlement, we used the vegetation departure index included within the LANDFIRE models. The vegetation departure index models the relative change in vegetated conditions from historical pre-European settlement conditions for each vegetated 30-meter pixel within the conterminous US. Reference conditions represent simulated historical vegetation composition and structure resulting from historical disturbance occurrence and severity [35]. LANDFIRE uses two models to develop historical reference conditions: 1) a Vegetation Dynamics Development Tool (VDDT) and 2) LANDSUM. VDDT is a quantitative state and transition model that combines information about the rates and pathways of vegetation development over time and the probabilities and effects of ecological disturbances. [36]. LANDSUM is a state and transition patch-level succession model combined with a spatially explicit disturbance model that simulates wildfire on a cell by cell basis [35]. The model uses outputs from the VDDT to quantify disturbance-succession patterns during the simulation period. This vegetation modeling framework is combined with estimates of climate and disturbance variability and used to simulate historical reference conditions for fire frequency and severity, and vegetation composition and structure [35].

To characterize current conditions, LANDFIRE generates Successional Class maps representing the current successional state of vegetation as determined by comparing LANDFIRE existing vegetation data products (current vegetation type, cover and height) with the defined successional composition and structure rules outlined by the VDDT [37]. Current conditions can then be compared to reference conditions for each pixel to determine a measure of departure. Only vegetative conditions are used in LANDFIRE, therefore areas of urban development and intensive agriculture are excluded from the model.

1.4. Proximity to aquatic resources

The importance of landscape linkages that enable energy transfer across terrestrial and aquatic ecosystems is well documented [38,39]. Terrestrial habitat condition is likely to be of higher quality in areas where proximity to freshwater resources exists. Aquatic insects, salmon [40], otters [41], birds [42], bats [43] and other organisms have been documented to transfer energy from aquatic to terrestrial land covers. Jackson and Fisher [44] first demonstrated the substantial impact of these exchanges, showing that emergent insect flux from a stream transferred more than 20 g/m2 of aquatic secondary production annually to terrestrial desert food webs. A growing body of literature now supports the hypothesis that streams subsidize food webs and energy transfer of terrestrial ecosystems, and that the magnitude of these subsidies can have large impacts [39,45].

While widely recognized as important, few studies have quantified the distance from aquatic systems into terrestrial land cover classes over which these "subsidies" operate, and most work has focused on streams rather than other systems [39,43,46–48]. We applied methods developed by Muehlbauer [39], who through meta-analysis demonstrated that a negative power function best matches observational data across a wide range of ecosystem types. Using a normalized aquatic subsidy curve adapted from [39] (Figure S3), we applied a weighted addition to the index of any pixel within one kilometer of a either a river, lake, or wetland.

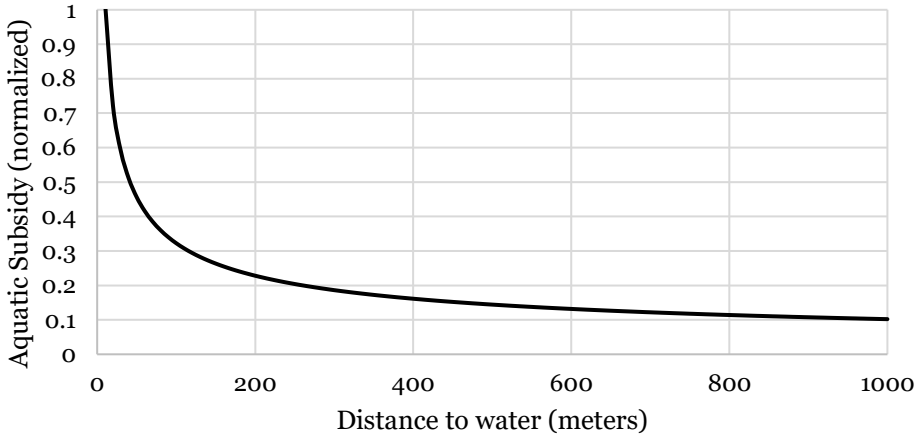

Figure S3. Normalized aquatic subsidies curve to be used to provide additional index weight to land cover classes within 1 kilometer of water. Curve adapted from [39].

2. Model Selection, Calibration, and Validation

We identified a dataset of ecological quality at 35,974 point locations throughout the CONUS. This dataset was created by collecting qualitative assessments based upon site visits FOR THE PURPOSE OF (NatureServe xxxx). Here each point location is graded from A (the best quality) to D (the worst) using an ordinal scale. The work that generated these points was conducted to assess the relative quality at sites already believed to have considerable natural habitat value. As such, the dataset appears biased, with a larger proportion of the points describing higher quality habitats (number of sites classified as A, B, C, and D are 10,675, 12,929, 8,588, and 3,782 respectively, see Figure S4 below). To address this bias in response data, we generated an additional 5,724 points that would likely be rated as the lowest quality (D) by selecting point locations outside, but within 100 meters of, high-density urban built up areas. Because ordinal response-based land cover datasets frequently prove problematic as a validation tool CITE), we elected to convert the four-category dataset into a binary response with zeros representing the poorer quality points (C & D) and ones representing higher quality (A & B).

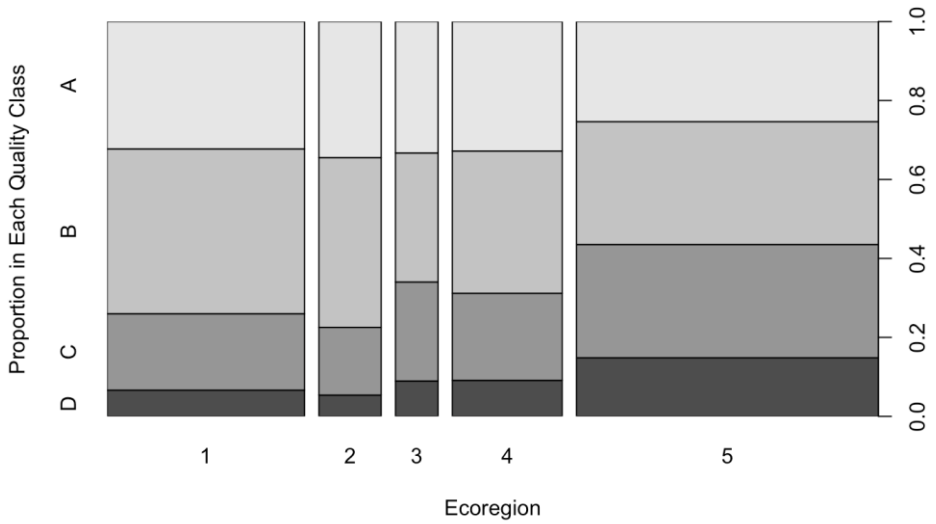

Figure S4. Number and proportion of validation points in each geographic region. Here, the width of each bar represents the relative number of points in each geographic region (1 through 5). The height of each shaded area within each region's bar describes the proportion of points rated at that quality level within each ecoregion. Ecoregions 1-5 are, respectively: Western Forest, Desert, Central Plains, Southeastern Forests, and Eastern/Northeastern Forests.

To prepare the HCI component layers, we z-transformed the four predictor layers (VDEP, ANTHRO, FRAG, and WATER) using the "scale" function in R [49]. Z-transformation normalizes datasets by subtracting the mean and dividing by the standard deviation, creating a scaled dataset where values are expressed as the number of standard deviations above or below the mean. This allows analysis where no data layer in a multivariate analysis has outsized predictive power simply due to differences in absolute values that might span orders of magnitude. Using validation points, we extracted values of each of the component HCI layers at these sites and added these to the validation dataset. We then converted this categorical validation dataset into a binary value (i.e., "0" for poor quality and "1" for high quality). The resulting dataset contained a binary response column, four HCI component predictor columns, and one column for the ecoregion (numbered from 1 to 5 (see Fig S.4)). We utilized 90% of these point locations, distributed randomly throughout the CONUS as calibration data. The remaining 10% of the data were withheld for model validation.

We then performed a comprehensive model selection to determine both the combinations of predictors and the relative weights for each of these predictors that best fit the response data. From the list of four possible predictors, we created a comprehensive model set, testing all combinations of predictors (and a null/intercept-only model) against the dataset of point location indicators of ecological integrity (N = 16 models). This step is necessary to identify any significant overfitting or between-layer correlation among the predictor variables.

Given potential autocorrelation between the component HCI layers (e.g., distance to anthropogenic structures and fragmentation are likely highly correlated), we hypothesized that some degree of overfitting may be unavoidable. However, we opted to test all possible combinations of predictor layers (n = 16) in the model selection process. To do this, we used a Bayesian framework within a loop, testing each of the 16 models separately using the BRMS package in R [50]. Here, the most likely parameter values for each layer in a given model are determined. The general goodness of fit of the models were then compared using Watanabe-Akaike Information Criteria (WAIC) and Leave-One-Out Cross-Validation (LOO) [51]. Model rank and posterior model probability (PMP, the probability that a given model is the best, most parsimonious model given the data) were then

determined using Bayesian bootstrap stabilized pseudo Bayesian model averaging (BB-pseudo-BMA, [52]).

We also hypothesized that the importance of predictor layers, and thus their coefficients, may vary from ecoregion to ecoregion based on known variation in the interaction of human and natural systems at this scale (e.g., proximity to aquatic habitat may constitute a larger ecological effect in more xeric areas or the significantly higher road density in the northeastern US compared to the western US). We therefore created an additional ecoregion variable dissecting the CONUS into five regions and created an additional 16 models with the same combinations of the HCI predictors as above, yet allowing for regionally varying coefficient values for each predictor.

We calculated the CONUS-scale HCI and regionally-varying HCI maps based upon the parameters of the best model in the CONUS and regional analyses respectively. To do this, we multiplied the parameter values for each of the HCI components from the respective best-fit models to each pixel of these component maps using the Raster Calculator function in ArcMap. Finally, we rescaled these datasets to a one to one-hundred scale to create an easy to interpret map of quality.

3. Results of the model selection / validation

Incorporation of by-ecoregion variation of coefficients for all for predictor variables (VDEP, ANTHRO, FRAG, and WATER) yielded the model with the highest posterior model probability (PMP = 0.9999, see supplemental Excel file, S2.PMP.xlsx for a comparison of all models. The parameters for the model are listed in the supplemental Excel file S3.bestfitmodel.xlsx. In Bayesian model averaging, as applied here, the total PMP summed over all test models must equal one, so the likelihood of any other model being the best predictor of the response data, or of contributing value to understanding of model fit is vanishingly small (probability < 0.001). Although the PMPs for all models excepting the best fit are exceedingly small, the ranking of models from best to worst fit still provides some information on relative value of each predictor variable. Of the 32 models tested, the 15 best fitting the response data all incorporated regional variation in the coefficient for each predictor, indicating the regional variation in each predictor's fit to the response. The only regionally varying model to rank lower than a CONUS-scale model was the regional null/intercept-only model.

Table S2. Posterior model probabilities for each of the tested models. Results show the probability that a given model is the best, most parsimonious model given the data (PMP). These results were generated after each model was run based on the model variables listed in the center column of this table in the Bayesian framework that allowed for binary (region) and continuous predictor variables (all others).

Model Number	Model Variables	PMP
m41.reg	Response ~ (VDEP + ANTHRO + FRAG + WATER | REGION)	0.999
m34.reg	Response ~ (ANTHRO + FRAG + WATER | REGION)	0.001
m31.reg	Response ~ (VDEP + ANTHRO + FRAG | REGION)	0.000
m33.reg	Response ~ (VDEP + FRAG + WATER | REGION)	0.000
m26.reg	Response ~ (FRAG + WATER | REGION)	0.000
m24.reg	Response ~ (ANTHRO + FRAG | REGION)	0.000
m22.reg	Response ~ (VDEP + FRAG | REGION)	0.000
m13.reg	Response ~ (FRAG | REGION)	0.000
m32.reg	Response ~ (VDEP + ANTHRO + WATER | REGION)	0.000
m21.reg	Response ~ (VDEP + ANTHRO | REGION)	0.000

m23.reg	Response ~ (VDEP + WATER | REGION)	0.000
m25.reg	Response ~ (ANTHRO + WATER | REGION)	0.000
m12.reg	Response ~ (ANTHRO | REGION)	0.000
m11.reg	Response ~ (VDEP | REGION)	0.000
m14.reg	Response ~ (WATER | REGION)	0.000
m33	Response ~ VDEP + FRAG + WATER	0.000
m41	Response ~ VDEP + ANTHRO + FRAG + WATER	0.000
regional.intercept	Response ~ (1 | REGION)	0.000
m31	Response ~ VDEP + ANTHRO + FRAG	0.000
m22	Response ~ VDEP + FRAG	0.000
m34	Response ~ ANTHRO + FRAG + WATER	0.000
m26	Response ~ FRAG + WATER	0.000
m13	Response ~ FRAG	0.000
m24	Response ~ ANTHRO + FRAG	0.000
m12	Response ~ ANTHRO	0.000
m14	Response ~ WATER	0.000
m21	Response ~ VDEP + ANTHRO	0.000
intercept	1	0.000
m25	Response ~ ANTHRO + WATER	0.000
m32	Response ~ VDEP + ANTHRO + WATER	0.000
m23	Response ~ VDEP + WATER	0.000
m11	Response ~ VDEP	0.000

Literature Cited for Supplemental Materials

1. Riitters, K.H.; Wickham, J.D.; Neill, R.V.O.; Jones, K.B.; Smith, E.R.; Coulston, J.W.; Wade, T.G.; Smith, J.H. Fragmentation of Continental United Forests. **2002**, *5*, 815–822, doi:10.1007/s10021002-0209-2.
2. Angermeier, P.L.; Karr, J.R. Biological Integrity Versus Biological Diversity as Policy Directives: Protecting Biotic Resources. In *Ecosystem Management: Selected Readings*; Samson, F.B., Knopf, F.L., Eds.; Springer New York: New York, NY, 1996; 264–275 ISBN 978-1-4612-4018-1.
3. Parrish, J.D.; Braun, D.P.; Unnasch, R.S. Are We Conserving What We Say We Are? Measuring Ecological Integrity within Protected Areas. *BioScience* **2003**, *53*, 851, doi:10.1641/0006-3568(2003)053[0851:AWCWWS]2.0.CO;2.
4. Spellerberg, I.F. Ecological Effects of Roads and Traffic: A Literature Review. *Global Ecology and Biogeography Letters* **1998**, *7*, 317–333, doi:10.2307/2997681.
5. Andrews, A. Fragmentation of Habitat by Roads and Utility Corridors: A Review. *Australian Zoologist* **2014**, *26*, 130–141, doi:10.7882/AZ.1990.005.
6. Gullison, R.; Hardner, J. The Effects of Road Design and Harvest Intensity on Forest Damage Caused by Selective Logging: Empirical Results and a Simulation Model from the Bosque Chimanes, Bolivia. **1993**, doi:10.1016/0378-1127(93)90067-W.
7. Reed, R.A.; Johnson-Barnard, J.; Baker, W.L. Contribution of Roads to Forest Fragmentation in the Rocky Mountains. *Conservation Biology* **1996**, *10*, 1098–1106, doi:10.1046/j.1523-1739.1996.10041098.x.
8. Forman, R.T.T.; Alexander, L.E. ROADS AND THEIR MAJOR ECOLOGICAL EFFECTS. *Annu. Rev. Ecol. Syst.* **1998**, *29*, 207–231, doi:10.1146/annurev.ecolsys.29.1.207.
9. Santos, A.M.; Tabarelli, M. Distance from Roads and Cities as a Predictor of Habitat Loss and Fragmentation in the Caatinga Vegetation of Brazil. *Braz. J. Biol.* **2002**, *62*, 897–905, doi:10.1590/S1519-69842002000500020.
10. van der Zande, A.N.; ter Keurs, W.J.; van der Weijden, W.J. The Impact of Roads on the Densities of Four Bird Species in an Open Field Habitat—Evidence of a Long-Distance Effect. *Biological Conservation* **1980**, *18*, 299–321, doi:10.1016/0006-3207(80)90006-3.
11. Reijnen, R.; Foppen, R.; Veenbaas, G. Disturbance by Traffic of Breeding Birds: Evaluation of the Effect and Considerations in Planning and Managing Road Corridors. *Biodiversity and Conservation* **1997**, *6*, 567–581, doi:10.1023/A:1018385312751.
12. Romin, L.; Bissonette, J. Temporal and Spatial Distribution of Highway Mortality of Mule Deer on Newly Constructed Roads at Jordanelle Reservoir, Utah. *Great Basin Naturalist* **1996**, *56*.
13. Boarman, W.; Sazaki, M. A Highway's Road-Effect Zone for Desert Tortoises (Gopherus Agassizii). *Journal of Arid Environments* **2006**, *65*, 94–101, doi:10.1016/j.jaridenv.2005.06.020.
14. Parris, K.; Schneider, A. Impacts of Traffic Noise and Traffic Volume on Birds of Roadside Habitats. *Ecology and Society* **2009**, *14*, doi:10.5751/ES-02761-140129.
15. Dunthorn, A.A.; Errington, F.P. Casualties among Birds along a Selected Road in Wiltshire. *Bird Study* **1964**, *11*, 168–182, doi:10.1080/00063656409476067.
16. Mclellan, B.; Shackleton, D.M. Immediate Reactions of Grizzly Bears to Human Activities. **1989**, *17*, 269–274.
17. Van Dyke, F.; Klein, W.C. Response of Elk to Installation of Oil Wells. *Journal of Mammalogy* **1996**, *77*, 1028–1041, doi:10.2307/1382783.
18. Mahoney, S.; Schaefer, J. Long-Term Changes in Demography and Migration of Newfoundland Caribou. *Journal of Mammalogy - J. MAMMAL* **2002**, *83*, 957–963, doi:10.1644/1545-1542(2002)083<0957:LTCIDA>2.0.CO;2.
19. Nellemann, C.; Vistnes, I.; Jordhøy, P.; Strand, O.; Newton, A. Progressive Impact of Piecemeal Infrastructure Development on Wild Reindeer. *Biological Conservation* **2003**, *113*, 307–317, doi:10.1016/S0006-3207(03)00048-X.
20. Barrios, L.; Rodríguez, A. Behavioural and Environmental Correlates of Soaring-Bird Mortality at on-Shore Wind Turbines. *Journal of Applied Ecology* **2004**, *41*, 72–81, doi:10.1111/j.1365-2664.2004.00876.x.
21. Hak, J.C.; Comer, P.J. Modeling Landscape Condition for Biodiversity Assessment—Application in Temperate North America. *Ecological Indicators* **2017**, *82*, 206–216, doi:10.1016/j.ecolind.2017.06.049.
22. Haila, Y. A Conceptual Genealogy of Fragmentation Research: From Island Biogeography to Landscape Ecology. *Ecological Applications* **2002**, *12*, 321–334, doi:10.2307/3060944.
23. Andrén, H. Effects of Habitat Fragmentation on Birds and Mammals in Landscapes with Different Proportions of Suitable Habitat: A Review. **1994**, *76*, 355–366, doi:10.2307/3545823.
24. Henle, K.; Davies, K.; Kleyer, M.; Margules, C.; Settele, J. Predictors of Species Sensitivity to Fragmentation. *Biodiversity and Conservation* **2004**, *13*, 207–251, doi:10.1023/B:BIOC.0000004319.91643.9e.
25. Cushman, S. Effects of Habitat Loss and Fragmentation on Amphibians: A Review and Prospectus. *Biological Conservation* **2006**, *128*, 231–240, doi:10.1016/j.biocon.2005.09.031.
26. Didham, R.; Ghazoul, J.; Stork, N.; Davis, A. Insects in Fragmented Forests: A Functional Approach. *Trends in ecology & evolution* **1996**, *11*, 255–260, doi:10.1016/0169-5347(96)20047-3.
27. Hobbs, R.J.; Yates, C.J. Impacts of Ecosystem Fragmentation on Plant Populations: Generalising the Idiosyncratic. *Australian Journal of Botany* **2003**, *51*, 471–488, doi:10.1071/BT03037.
28. Riitters, K.H.; O'Neill, R.V.; Hunsaker, C.T.; Wickham, J.D.; Yankee, D.H.; Timmins, S.P.; Jones, K.B.; Jackson, B.L. A Factor Analysis of Landscape Pattern and Structure Metrics. *Landscape Ecol* **1995**, *10*, 23–39, doi:10.1007/BF00158551.
29. Vogelmann, J.E. Assessment of Forest Fragmentation in Southern New England Using Remote Sensing and Geographic Information Systems Technology. *Conservation Biology* **1995**, *9*, 439–449.
30. Trani, M.K.; Giles, Rhj. An Analysis of Deforestation: Metrics Used to Describe Pattern Change. *For. Ecol Manage.* **1999**, *114*, 459–470, doi:10.1016/s0378-1127(98)00375-2.

31. Wickham, J.D.; Jones, K.B.; Riitters, K.H.; Wade, T.G.; O'Neill, R.V. Transitions in Forest Fragmentation: Implications for Restoration Opportunities at Regional Scales. *Landscape Ecology* **1999**, *14*, 137–145, doi:10.1023/A:1008026129712.
32. Mcgarigal, K.; Cushman, S.A. Comparative Evaluation of Experimental Approaches to the Study of Habitat Fragmentation Effects. *Ecological Applications* **2002**, *12*, 11.
33. Cushman, S.A.; McGarigal, K. Landscape Metrics, Scales of Resolution. In *Designing Green Landscapes*; von Gadow, K., Pukkala, T., Eds.; Managing Forest Ecosystems; Springer Netherlands: Dordrecht, 2008; Vol. 15, pp. 33–51 ISBN 978-1-4020-6758-7.
34. Hurd, J.D.; Civco, D.L. Assessing Forest Fragmentation in Connecticut Using Multi-Temporal Land Cover. *San Diego* **2010**, 11.
35. Pratt, S.; Holsinger, L.; Keane, R.E. Chapter 10 - Using Simulation Modeling to Assess Historical Reference Conditions for Vegetation and Fire Regimes for the LANDFIRE Prototype Project. *In: Rollins, Matthew G.; Frame, Christine K., tech. eds. 2006. The LANDFIRE Prototype Project: Nationally consistent and locally relevant geospatial data for wildland fire management Gen. Tech. Rep. RMRS-GTR-175. Fort Collins: U.S. Department of Agriculture, Forest Service, Rocky Mountain Research Station. p. 277-314* **2006**, *175*.
36. Beukema, S.J.; Reinhardt, E.D.; Greenough, J.A.; Robinson, D.C.E.; Kurz, W.A. Chapter 2: Fire and Fuels Extension: Model Description. *In: Reinhardt, Elizabeth; Crookston, Nicholas L. (Technical Editors). The Fire and Fuels Extension to the Forest Vegetation Simulator. Gen. Tech. Rep. RMRS-GTR-116. Ogden, UT: U.S. Department of Agriculture, Forest Service, Rocky Mountain Research Station. p. 11-60.* **2003**, *116*.
37. Rollins, M.G.; Frame, C.K. *The LANDFIRE Prototype Project: Nationally Consistent and Locally Relevant Geospatial Data for Wildland Fire Management*; U.S. Department of Agriculture, Forest Service, Rocky Mountain Research Station: Ft. Collins, CO, 2006; p. RMRS-GTR-175;.
38. Polis, G.; Power, M.; Huxel, G. Food Webs at the Landscape Level. *Bibliovault OAI Repository, the University of Chicago Press* **2001**.
39. Muehlbauer, J.D.; Collins, S.F.; Doyle, M.W.; Tockner, K. How Wide Is a Stream? Spatial Extent of the Potential "Stream Signature" in Terrestrial Food Webs Using Meta-Analysis. *Ecology* **2014**, *95*, 44–55, doi:10.1890/12-1628.1.
40. Helfield, J.; Naiman, R. Effects of Salmon-Derived Nitrogen on Riparian Forest Growth and Implications for Stream Productivity. *Ecology* **2001**, *82*, 2403–2409, doi:10.1890/0012-9658(2001)082[2403:EOSDNO]2.0.CO;2.
41. Ben-David, M.; Bowyer, R.T.; Duffy, L.K.; Roby, D.D.; Schell, D.M. Social Behavior and Ecosystem Processes: River Otter Latrines and Nutrient Dynamics of Terrestrial Vegetation. *Ecology* **1998**, *79*, 2567–2571, doi:10.1890/0012-9658(1998)079[2567:SBAEPR]2.0.CO;2.
42. Bueno, A.; Bruno, R.; Pimentel, T.; Sanaiotti, T.; Magnusson, W. The Width of Riparian Habitats for Understory Birds in an Amazonian Forest. *Ecological applications : A publication of the Ecological Society of America* **2012**, *22*, 722–734, doi:10.2307/41416795.
43. Power, M.; Rainey, W.; Parker, M.; Sabo, J.; Smyth, A.; Khandwala, S.; Finlay, J.; Mcneely, C.; Marsee, K.; Anderson, C. River-to-Watershed Subsidies in an Old-Growth Conifer Forest. *Food Webs at the Landscape Level* **2004**, 217–240.
44. Jackson, J.K.; Fisher, S.G. Secondary Production, Emergence, and Export of Aquatic Insects of a Sonoran Desert Stream. *Ecology* **1986**, *67*, 629–638, doi:10.2307/1937686.
45. Baxter, C.V.; Fausch, K.D.; Carl Saunders, W. Tangled Webs: Reciprocal Flows of Invertebrate Prey Link Streams and Riparian Zones: Prey Subsidies Link Stream and Riparian Food Webs. *Freshwater Biology* **2005**, *50*, 201–220, doi:10.1111/j.1365-2427.2004.01328.x.
46. Sanzone, D.M.; Meyer, J.L.; Marti, E.; Gardiner, E.P.; Tank, J.L.; Grimm, N.B. Carbon and Nitrogen Transfer from a Desert Stream to Riparian Predators. *Oecologia* **2003**, *134*, 238–250, doi:10.1007/s00442-002-1113-3.
47. Briers, R.A.; Biggs, J. Spatial Patterns in Pond Invertebrate Communities: Separating Environmental and Distance Effects. *Aquatic Conserv: Mar. Freshw. Ecosyst.* **2005**, *15*, 549–557, doi:10.1002/aqc.742.
48. Raikow, D.F.; Walters, D.M.; Fritz, K.M.; Mills, M.A. The Distance That Contaminated Aquatic Subsidies Extend into Lake Riparian Zones. *Ecol Appl* **2011**, *21*, 983–990, doi:10.1890/09-1504.1.
49. R Core Team *R: A Language and Environment for Statistical Computing.*; R Foundation for Statistical Computing: Vienna, Austria;.
50. Bürkner, P.-C. Brms: An R Package for Bayesian Multilevel Models Using Stan. *Journal of Statistical Software* **2017**, *80*, 1–28, doi:10.18637/jss.v080.i01.
51. Vehtari, A.; Gelman, A.; Gabry, J. Practical Bayesian Model Evaluation Using Leave-One-out Cross-Validation and WAIC. *Stat. Comput* **2017**, *27*, 1413–1432, doi:10.1007/s11222-016-9696-4.
52. Yao, Y.; Vehtari, A.; Simpson, D.; Gelman, A. Using Stacking to Average Bayesian Predictive Distributions (with Discussion). *Bayesian Anal.* **2018**, *13*, doi:10.1214/17-BA1091.